Research Article

Journal of Molecular Recognition

Received: 31 October 2013, Accepted: 2 December 2013, Published online in Wiley Online Library

(wileyonlinelibrary.com) DOI: 10.1002/jmr.2346

Binding of azurin to cytochrome *c* 551 as investigated by surface plasmon resonance and fluorescence

Simona Santini[a], Anna Rita Bizzarri[a]*, Tohru Yamada[b], Craig W. Beattie[b] and Salvatore Cannistraro[a]

The interaction between azurin (Az) and cytochrome *c* 551 (CytC551) from *Pseudomonas aeruginosa* deserves particular interest for both its physiological aspects and their possible applications in bionano devices. Here, the kinetics of the interaction has been studied by surface plasmon resonance and fluorescence quenching. Surface plasmon resonance data have been successfully interpreted by the heterogeneous ligand model, which predicts the existence of two binding sites on the immobilized Az for CytC551 molecules in solution. On the other hand, the fluorescence study indicates the formation of a complex, with the involvement of the lone Az tryptophan (Trp) at position 48. The two different techniques point out the occurrence of an encounter complex between Az and CytC551 that evolves toward the formation of a more stable complex characterized by an equilibrium dissociation constant K_D typical of transient interactions. Copyright © 2014 John Wiley & Sons, Ltd.

Keywords: electron transfer proteins; blue copper proteins; biosensors; complex kinetics

INTRODUCTION

Redox metalloproteins have gained in recent years a particular interest for their application in molecular bionanoelectronics (Gorton *et al*., 1999; Willner and Willner, 2001; Adams *et al*., 2003; Jain, 2005; Guo and Dong, 2009; Prabhulkar *et al*., 2012). Their very efficient electron transfer (ET) capability, as well as their property of recognizing the partner in a specific way (Janin, 2000), can be combined with the progress of microelectronics and nano-electronics to create hybrid systems to use as fast and sensitive biosensors (Marvin and Hellinga, 2001; Andolfi and Cannistraro, 2005; Bonanni *et al*., 2005). The ET process occurring between a metalloprotein, coupled with an electrode, and its partner in solution, requires a specific biorecognition event promoting the formation of a complex, likely characterized by a transient interaction and by a high physiological turnover. Indeed, equilibrium dissociation constants ($K_D = k_{off}/k_{on}$) in the 10^{-3}–10^{-6} M range have been registered for these complexes (Crowley and Ubbink, 2003; Nooren and Thornton, 2003).

Among ET proteins, blue copper proteins deserve particular interest (Solomon *et al*., 1992) They are biomolecules acting as mobile electron carriers in a variety of biological processes, where the ET deeply involves the active site containing a copper ion, switching between the Cu^+ and Cu^{2+} state. Within the active site, the Cu ion is coordinated to a number of the protein ligands, according to a particular tetrahedral geometry, which endows the biomolecule with a finely tuneable ET mechanism, rendering them good candidates for application in biosensors.

In particular, Az (Nar *et al*., 1991; Solomon *et al*., 1992; Arcangeli *et al*., 1999; Webb and Loppnow, 1999), a 128 amino acids blue copper protein, which is part of the respiratory chain of the denitrifying bacteria *Pseudomonas aeruginosa*, is one of the most attractive ET proteins for its peculiar optical and spectroscopic properties (Sykes, 1991; Webb and Loppnow, 1999; Cimei *et al*., 2002). In addition, the protein has attracted growing interest for its prominent anticancer role consequent to its interaction with the tumor suppressor p53 (Yamada *et al*., 2002; Taranta *et al*., 2008) and perhaps involving oxygen reactive species generation (Liu *et al*., 2008; Bizzarri *et al*., 2012).

The physiological partner of Az is CytC551 (Matsuura *et al*., 1982; Gray and Winkler, 1996; Cutruzzolà *et al*., 2002; Ceruso *et al*., 2003), a monomeric heme protein of 82 amino acids organized in four α-helixes. Several experimental evidences of an ET process occurring between Az and CytC551 have been provided (Wilson *et al*., 1975; Silvestrini *et al*., 1982; Zannoni, 1989; Cutruzzolà *et al*., 2002). Moreover, the formation of an Az–CytC551 complex, whose existence has been under debate for decades (Cutruzzolà *et al*., 2002), has been recently modeled by computational methods and then experimentally supported. In particular, docking and molecular dynamics simulations (Bizzarri *et al*., 2007; Bizzarri, 2011) have predicted the best structure of the complex (Figure 1(a)). On the other hand, the complex has been investigated at single molecule level by atomic force spectroscopy, which has allowed the determination of the protein–protein interaction force and the dissociation rate

* *Correspondence to: Anna Rita Bizzarri, Biophysics and Nanoscience Centre, CNISM, Dipartimento DEB, Università della Tuscia, Viterbo, Italy.*
E-mail: bizzarri@unitus.it

a *S. Santini, A. R. Bizzarri, S. Cannistraro*
Biophysics and Nanoscience Centre, CNISM, Dipartimento DEB, Università della Tuscia, Viterbo, Italy

b *T. Yamada, C. W. Beattie*
Department of Surgery, Division of Surgical Oncology, University of Illinois, Chicago, IL, USA

Copyright © 2014 John Wiley & Sons, Ltd.

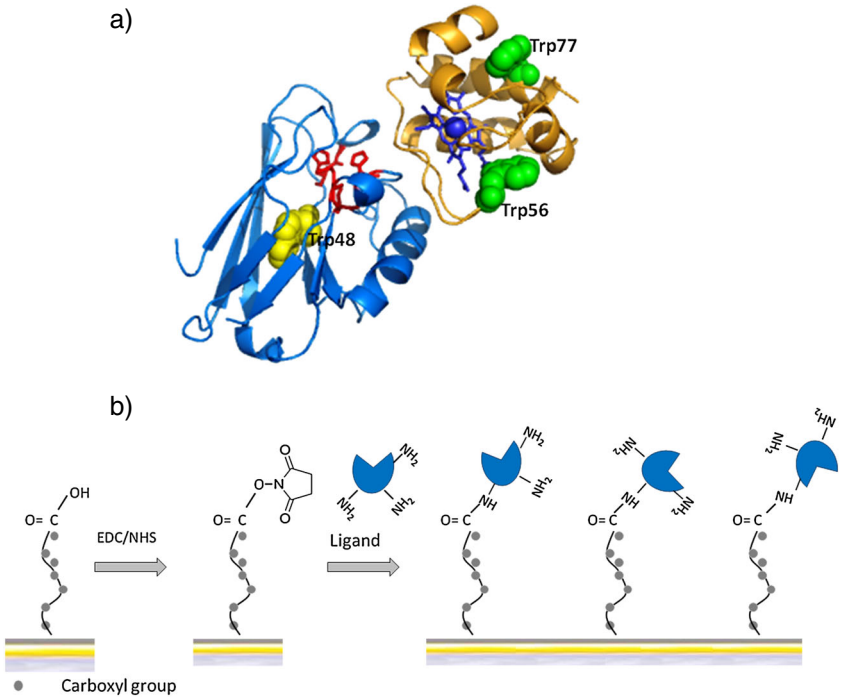

Figure 1. a) Three dimensional structure of the best complex between Az (blue) and CytC551 (orange) as predicted by the computational docking study reported in ref. 30. Az and CytC551 redox centers are shown as red and violet sticks, respectively. Az Trp48 is shown as yellow spheres, whereas green spheres in CytC551 represent its Trp77 and Trp56. b) Scheme of the immobilization strategy used in the SPR approach. First, the CM5 carboxymethylated dextran is activated by an EDC/NHS mixture, then the ligand (Az) is fluxed over the surface. The ligand immobilized through the NH_2 group of Lys residues is expected to be randomly oriented.

for different immobilization strategies (Bonanni *et al*., 2005; Bonanni *et al*., 2006). However, the complex has not been completely characterized from a kinetic point of view. This would be conversely quite insightful for the elucidation of the ET mechanism and crucial for using the Az–CytC551 system in bioelectronic devices.

In this work, the Az–CytC551 interaction has been studied with surface plasmon resonance (SPR) and fluorescence quenching spectroscopy. SPR has emerged as a strategic tool especially suited for sensitive kinetic investigation, in real time and without any labeling, of binding processes between a molecule anchored to a substrate and its partner free in solution (Homola *et al*., 1999; Cooper, 2003). On the other hand, fluorescence quenching is a powerful technique to study protein–protein interactions involving tryptophan or tyrosine residues when both the partners are free in solution, as it happens in physiological conditions (Lakowicz, 2006). The binding kinetics obtained by adding progressively higher concentrations of CytC551 to an Az-containing sample has been followed by both the two approaches. The experimental data, analyzed even in terms of several binding models, have pointed out the occurrence of a specific complex between Az and CytC551, whose equilibrium dissociation constant K_D is consistent with transient interaction features.

EXPERIMENTAL METHODS

Protein expression and purification

Azurin from *P. Aeruginosa* was purchased from Sigma Aldrich (St. Louis, Mo) and used without further purification.

Recombinant CytC551 was purified as described previously (Goto *et al*., 2003; Hiraoka *et al*., 2004). *Escherichia coli* JCB7120 was used as a host strain for expression of cytochrome c_{551}-encoding gene of *P. Aeruginosa*. The transformed *E. coli* cells were cultivated under anaerobic conditions at 37 °C in the minimal medium as described (Hasegawa *et al*., 1999). Periplasmic protein fractions were collected by cold osmotic shock. The CytC551 in the periplasmic fraction were purified by ÄKTAprime plus FPLC system (GE Healthcare), and protein concentrations were determined by the Bio-Rad protein assay kit (Bio-Rad, Hercules, CA) with bovine serum albumin as a standard. The purity of CytC551 were assessed on SDS-PAGE gels stained with Coomassie Brilliant Blue and also immune blotting with polyclonal anti-CytC551 antibody (Hiraoka *et al*., 2004).

Surface plasmon resonance measurements

Surface plasmon resonance measurements were performed at 25 °C using a Biacore X100 instrument (GE Healthcare, Bio-Sciences AB, Sweden). Experiments were carried out in 50-mM PBS buffer pH 7.5 filtered with a 0.22-μM membrane filter, to which surfactant P20 0.005% (GE Healthcare) was added. Other reagents were all provided by GE Healthcare: CM5 sensor chip; Biacore Amine coupling Kit including N-hydroxyl-succinimide (NHS), N-ethyl-N-(3-diethylaminopropyl) carbodiimide (EDC) and ethanolamine hydrochloride 1 M pH 8.5; acetate buffer pH 4 used as immobilization buffer; washing buffer SDS 0.05%.

In SPR measurements, Az molecules (ligand) were immobilized to a single channel of a CM5 sensor chip surface by targeting the amine groups of the lysine residues exposed on the protein surface.

To this aim, the standard amine coupling procedure (Figure 1(b)) was used according to the manufacturer's instructions. Briefly, the COOH groups of the carboxymethylated dextran in the sensor chip were converted to active esters by mixing 100 μl 0.4 M EDC with

 Copyright © 2014 John Wiley & Sons, Ltd.

100 μl 0.1 M NHS from the amine coupling kit and injecting the mixture into the instrument at a flow rate of 10 μl/min for 7 min. The solution of Az, eluted up to a final concentration of about 0.06 μg/μl in 10 mM acetate buffer pH 4, was then injected over the activated surface until an immobilization level of about 200 resonance units (RU) was reached. Once the immobilization procedure was completed, nonspecifically bound proteins were removed by washing with running buffer until the RU value became nearly constant. Unreacted sites on the sensor chip were then masked by injecting 1 M ethanolamine-HCl pH 8.5 for 7 min at flow rate of 10 μl/min. Running buffer was fluxed over the surface until the baseline was stable. The second (or reference) flow cell was instead activated and deactivated without coupling Az and used as a control surface for refractive index change and no specific binding.

Experiments were conducted via sequential injection of five flushes of CytC551 solution with increasing concentrations from 0.5 to $50{\cdot}10^{-6}$ M in running buffer flushed on the sensor chip surface at a flow rate of 30 μl/min for 120 s, followed by a 10-min dissociation time without intermediate regeneration. Analytical cycles were programmed by means of a wizard template, and the entire analysis was completely automated.

Experimental curves (sensorgrams) were double-reference subtracted (Myszka, 1999). In other words, the response collected over the functionalized surfaces was subtracted by the response from the reference surface to correct for bulk refractive index changes. Then, the response from an average of blank injections was subtracted from the experimental response to remove any systematic artifact arising from the reaction flow and the reference cells.

The curves were then analyzed by nonlinear curve fitting of the entire data set with the BIAevaluation 2.0 software (GE Healthcare Bio-Sciences AB, Sweden). Fits were evaluated by visual inspection, χ^2 values, *T*-values, and observation of residual plot. They were accepted when χ^2 was <10, *T* value was >10, and when residuals were randomly distributed in a band as close as possible.

We also tried to covalently link CytC551 instead of Az to the chip according to the same amine coupling procedure described in the previous text. However, we did not reach the RU level necessary to perform a reliable kinetic study, this being likely a consequence of the unfavorable number and exposition of lysine residues on the CytC551 surface.

Steady-state fluorescence quenching measurements

Tryptophan fluorescence emission spectra were recorded at room temperature by a Spex FluoroMax (Jobin Yvon, France) spectrofluorimeter, equipped with a XBO 150 W Xenon lamp (OSRAM GmbH, Munich, Germany). Samples were excited by a 290-nm wavelength (3-nm excitation bandwidth) so that excitation of tyrosine residues and energy transfer to the lone indole side chain were minimized. The light emitted by 500 μl of sample kept in a 0.2×1.0-cm internal size quartz cuvette was collected at right angle to the excitation radiation and scanned from 300 to 450 nm (3-nm emission bandwidth). An integration time of 1.0 s, related to 0.5 nm step, was used. Az sample 10 μM in sodium acetate buffer pH 4.6 was titrated with CytC551 at a final concentration ranging between 0 and 200 μM. The change in fluorescence emission intensity was measured within 1 min after adding CytC551 to Az. Appropriate blanks corresponding to the buffer were subtracted to correct for Raman scattering background.

RESULTS AND DISCUSSION

Surface plasmon resonance binding experiments

The interaction kinetics between CytC551 and Az has been studied by the SPR kinetic titration approach in which the analyte and the buffer solution are alternately injected into the cell containing the chip where the ligand has been immobilized (Karlsson *et al.*, 2006). Such an approach is faster than the classical one because it does not require a complete regeneration of the chip before each analyte injection. Furthermore, the immobilized target last longer and the ligand activity is fully preserved, this resulting in an increased efficiency and reduction of costs.

The resulting sawtooth SPR profile obtained from the successive injections of CytC551 solution at five progressively higher concentrations on the cell with Az is shown in Figure 2 (continuous line). After the first injection with the CytC551 solution, the signal increases nonlinearly and approaches a plateau. At the end of the first CytC551 injection (see the arrow in Figure 2), the buffer is flowed over the ligand and the signal drops down, followed by a slow decreasing trend down to zero until the successive CytC551 injection. Progressively higher signals are obtained as far as higher CytC551 concentrations are used. The inset of Figure 2, showing the binding isotherms for bare CytC551 with no ligand (Az) immobilized on the surface, displays a negligible increase of the baseline signal with respect to that observed on the cell with Az (about 2 RUs). This indicates that the progressive signal increase is due to a specific interaction of CytC551 to Az molecules immobilized on the chip. On the other hand, each buffer injection yields a decrease of the signal down to an almost constant value different from zero and more and more higher at each step, this being ascribed to a partial dissociation of the previously formed complexes on the chip.

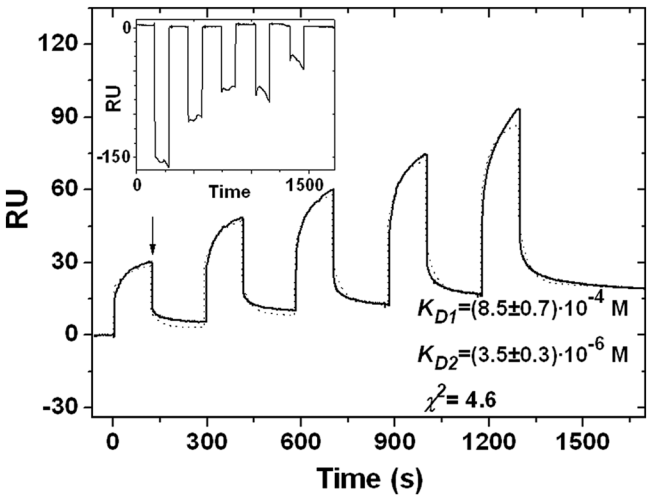

Figure 2. Surface plasmon resonance sensorgram for the association and dissociation of CytC551 on Az-modified sensor chip surface (continuous line). The fit has been obtained by the heterogeneous ligand model (dashed line). The arrow indicates the first injection of the buffer. The global fitting procedure by Eq. 3–6 provided the following values for the k_{on} and k_{off} of the interaction: $k_{on1} = (2.23 \pm 0.14)\ 10^2\ M^{-1}\ s^{-1}$; $k_{off1} = (1.90 \pm 0.05)\ 10^{-1}\ s^{-1}$; $k_{on2} = (3.04 \pm 0.10)\ 10^2\ M^{-1}\ s^{-1}$; $k_{off2} = (1.07 \pm 0.07)\ 10^{-3}\ s^{-1}$. Inset: the binding isotherms for CytC551 with no ligand (Az) immobilized on the surface.

Copyright © 2014 John Wiley & Sons, Ltd.

Journal of Molecular Recognition

To extract information on the affinity between CytC551 and Az, we have analyzed the SPR data by fitting the whole SPR profile with several kinetic models by a nonlinear least square analysis (Morton *et al*., 1995). In particular, we have taken into account the classical Langmuir one-to-one, the heterogeneous ligand, the heterogeneous analyte, and the two-state binding models (Schasfoort and Tudos, 2008).

The Langmuir 1:1, or single-step binding model, provides the simplest approach to describe a ligand–analyte interaction, assuming a 1:1 interaction between the ligand (L), and the analyte (A) (O'Shannessy *et al*., 1993; Björquist and Boström, 1997). Such a model can be described by the following reaction equation:

$$L + A \underset{k_{off}}{\overset{k_{on}}{\rightleftarrows}} LA \tag{1}$$

where k_{on} and k_{off} are the association and dissociation rates of the complex respectively, with the corresponding K_D being given by k_{off}/k_{on}. Here, the analyte is CytC551 and the ligand is Az. However, the best fit by this model does not allow us to reach a satisfactory description of SPR data with a χ^2 value higher than 10 ($\chi^2 = 12.6$, not shown).

Similarly, both the heterogeneous analyte model and the two-state binding model were found not suitable to fit the experimental sensorgrams (data not shown). The former assumes that there are two independent reactions involving two different sites on the analyte (Karlsson, 1994), whereas the latter accounts for some conformational changes of the molecules upon forming complex (De Crescenzo *et al*., 2000). A good description of our SPR data has been instead obtained by the heterogeneous ligand model, which assumes the presence on the ligand of two binding sites (L_1 and L_2), each one binding one analyte molecule with different affinity (O'Shannessy and Winzor, 1996). Accordingly, the binding process can be described by

$$L_1 + A \underset{k_{off1}}{\overset{k_{on1}}{\rightleftarrows}} L_1A \text{ and } L_2 + A \underset{k_{off2}}{\overset{k_{on2}}{\rightleftarrows}} L_2A \tag{2}$$

where k_{onn} and k_{offn} ($n = 1$ or 2) are the association and dissociation rates for the corresponding reactions, 1 or 2. The model is described by the following differential equations:

$$d[L_1]/dt = -(k_{on1} \cdot [L_1] \cdot [A] - k_{off1} \cdot [L_1A]) \tag{3}$$

$$d[AL_1]/dt = k_{on1} \cdot [L_1] \cdot [A] - k_{off1} \cdot [L_1A] \tag{4}$$

$$d[L_2]/dt = -(k_{on2} \cdot [L_2] \cdot [A] - k_{off2} \cdot [L_2A]) \tag{5}$$

$$d[AL_2]/dt = k_{on2} \cdot [L_2] \cdot [A] - k_{off2} \cdot [L_2A] \tag{6}$$

The best fit of the SPR data in the framework of this model is shown in Figure 2 (dashed line) together with its χ^2 value and the K_D extracted for each ligand binding site. Association and dissociation rate constants of the interaction have been also extracted for each one of the two binding events. Specifically, we have found $k_{on1} = (2.23 \pm 0.14)\ 10^2\ M^{-1}\ s^{-1}$; $k_{off1} = (1.90 \pm 0.05)\ 10^{-1}\ s^{-1}$; $k_{on2} = (3.04 \pm 0.10)\ \ 10^2\ M^{-1}\ s^{-1}$; $k_{off2} = (1.07 \pm 0.07)\ 10^{-3}\ s^{-1}$. The good χ^2 obtained ($\chi^2 = 4.6$), the K_Ds values, and the sensorgram tendency toward a plateau indicate the formation of a complex between Az and CytC551 with a kinetics deviating from the pseudo-first order and involving two different Az binding sites. The K_{D1} dissociation constant, $K_{D1} = k_{off1}/k_{on1} = (8.5 \pm 0.7) \cdot 10^{-4}$ M, is significantly higher than the values usually observed for biomolecular complexes, which range from 10^{-12} M for complexes characterized by an extremely high affinity, to 10^{-5} M for complexes with a very low affinity, including transient complexes (Ubbink, 2009). Accordingly, reaction 1 may correspond to an encounter interaction between the partners, which likely does not give rise to the formation of a stable complex. Conversely, the second reaction, which is characterized by a lower dissociation constant $K_{D2} = k_{off2}/k_{on2} = (3.5 \pm 0.3) \cdot 10^{-6}$ M, could correspond to an interaction between CytC551 and Az typical of transient complexes. We note on passing that a dissociation constant of about 10^{-6} M has been obtained by SPR for a complex involving cytochrome c molecule and neuroglobin (Bønding *et al*., 2008). The existence of two Az binding sites for the interaction with CytC551 can be interpreted in terms of the so-called encounter complex model, which is often used to describe the formation of transient complexes between ET biomolecules (Marcus and Sutin, 1985; Crowley and Ubbink, 2003; Ubbink, 2009). Briefly, the binding process between two molecules takes place involving different steps: first, the two biomolecules form an encounter complex typically guided by long range electrostatic forces; then, they undergo rotational, vibrational, and diffusional motions, giving rise to a specific reactive interaction. Once this complex is formed, an ET process between the molecules takes place, followed by a dissociation of the complex itself to yield the products (Ubbink, 2009). Such a view could be consistent with the observation of two interaction sites, one with a low affinity, related to the formation of the encounter complex, and another one characterized by a much higher affinity, which describes the final complex between the molecules. However, we cannot rule out that the heterogeneity of the ligand immobilized on the chip could be responsible for the existence of two binding interactions (Catimel *et al*., 1997). Indeed, because Az is bound to the dextran matrix of a CM5 chip through amino groups attachment, the protein will be randomly oriented over the chip surface (Figure 1(b)). Consequently, it could be likely that a subpopulation of bound molecules are oriented in such a way that they can have a different affinity for the partner or even they cannot participate in the binding reaction with CytC551. Accordingly, the two binding interactions could arise from the contribution of a weighted average of complexes with different affinity. Such a picture has been used to explain results from SPR experiments with a similar anchoring procedure (De Crescenzo *et al*., 2000).

Fluorescence quenching experiment

To get additional insight on the interaction between CytC511 and Az, we have followed the fluorescence emission of an Az solution, excited at a 290-nm wavelength after the addition of progressively higher concentrations of CytC551. When bare Az molecules in solution (10 μM) are excited at 290-nm wavelength, the corresponding emission spectrum is characterized by a peak at about 308 nm (see the black dashed line in Figure 3). Such a signal arises from the emission of the lone Az Trp (Trp48) (Turoverov *et al*., 1985; Nar *et al*., 1991; Delfino and Cannistraro, 2009), which is located in a highly hydrophobic environment (Figure 1(a)). At the same excitation wavelength, the fluorescence emission spectrum of CytC551 shows a broad peak centered at about 348 nm (see the inset of Figure 3) (Borgia *et al*., 2008). Such a signal arises from the two CytC551 Trp residues, Trp77 and Trp56, the former occupying a marginal position with respect to

 Copyright © 2014 John Wiley & Sons, Ltd.

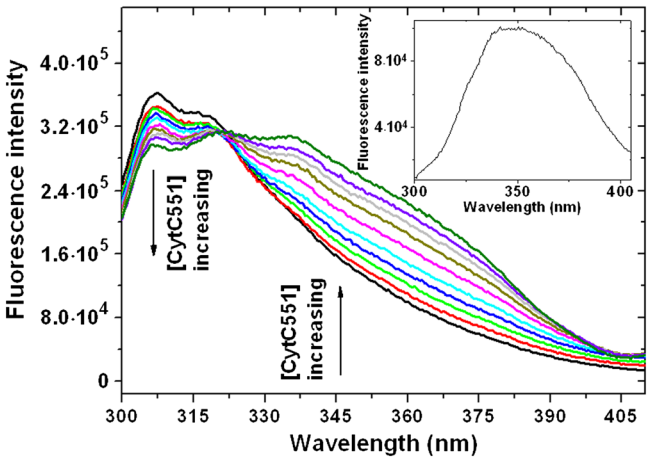

Figure 3. Representative fluorescence spectra of 10 μM Az in sodium acetate buffer pH 4.6 titrated by increasing CytC551 concentrations. Appropriate blanks corresponding to the buffer were subtracted to correct for Raman background. A quenching of the Az emission fluorescence of about 1.6% resulting from the dilution of the protein after CytC551 addition has been considered and carefully added to the experimental spectra. Inset: fluorescence spectrum of CytC551 8.7 μM in acetate buffer pH 4.6 excited at 290 nm.

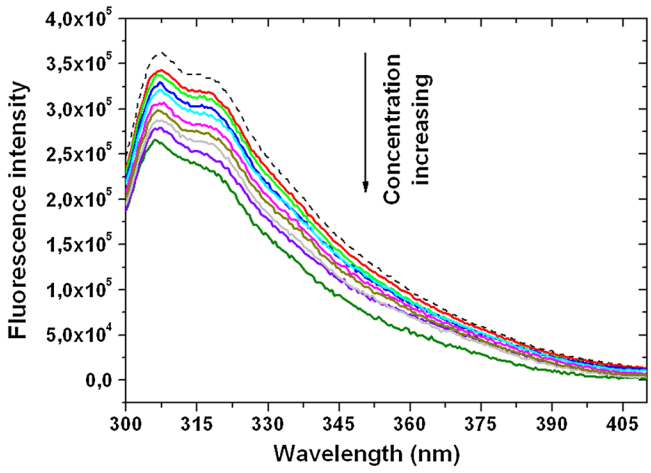

Figure 4. Fluorescence spectra showed in Figure 3 subtracted by the contribution of CytC551 to the fluorescence.

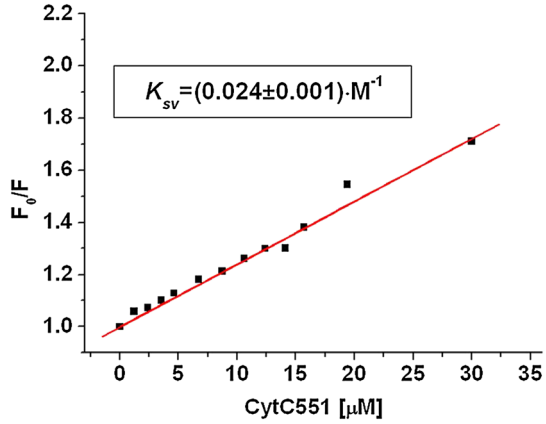

Figure 5. Stern–Volmer plot of Az fluorescence quenching as a function of CytC551 concentration. Continuous red line is the linear fit by Eq.7; the value of K_{SV} extracted from the fit being reported.

the hydrophobic core of the protein and the latter being buried inside it (Borgia *et al.*, 2008) (Figure 1(a)). Because CytC551 Trps emission is situated well apart from that of the Az Trp, it is possible to distinguish the emission peak of Az Trp48 from that of CytC551 in the mixed solution. Fluorescence emission spectra of Az titrated with CytC551 up to 15.7 μM are shown in Figure 3. The intensity of the fluorescence peak at 308 nm, arising from the Az Trp48, is progressively reduced upon the addition of CytC551, without any wavelength shift of the maximum. At the same time, the fluorescence emission intensity at around 348 nm increases with the CytC551 concentration. The fluorescence quenching of Az Trp48 is shown in Figure 4, where the spectra of Figure 3 have been carefully subtracted by the contribution of CytC551 to the fluorescence emission spectrum.

The quenching of the fluorescence emission at 308 nm after addition of CytC551 indicates a molecular interaction of CytC551 with Az, somewhat involving the lone Az Trp residue. It would be interesting therefore to ascertain if a dynamic or static process is responsible for such quenching—in other words, if the quenching just arises from collisional encounters between the molecules and then is dynamically controlled by diffusion, or, instead, by the formation of a specific complex between the two biomolecules, involving Trp48 of Az (Lakowicz, 1999).

The fluorescence quenching data have been thus analyzed by applying the Stern–Volmer equation given by

$$\frac{F_0}{F} = 1 + k_q \tau_q [Q] = 1 + K_{SV}[Q] \qquad (7)$$

where F_0 and F are the fluorescence intensities in the absence and presence of the quencher, respectively, k_q is the bimolecular quenching constant (or quenching rate constant), K_{SV} is the Stern–Volmer quenching constant of the interaction, providing information on the binding affinity, [Q] is CytC551 concentration, and τ_q is the average lifetime of the fluorophore in the absence of quencher.

The Stern–Volmer plot of F_0/F versus CytC551 concentrations up to 30 μM is shown in Figure 5. At higher CytC551 concentrations, the broad CytC551 emission peak centered at about 348 nm completely masks the Az Trp48 emission at 308 nm making the extraction of the F_0/F values practically unreliable. The plot reveals a linear trend which can be traced back to the involvement of a single Trp in the interaction with the quencher (Figure 5). From the slope of the linear fit by Eq. 7, we have determined the Stern–Volmer quenching constant $K_{SV} = (0.024 \pm 0.001) \cdot 10^6\ M^{-1}$; the bimolecular quenching constant $k_q = K_{SV}/\tau_q$ can be also extracted upon estimating τ_q. A reasonable value for τ_q has been reported to be about 10^{-9} s (Lakowicz, 1999). Using such a value, we found that k_q turns out to be about $10^{13}\ M^{-1}\ s^{-1}$, which is much higher than the limiting diffusion constant K_{diff} of the biomolecule (K_{diff} is about $2{\cdot}10^{10}\ M^{-1}\ s^{-1}$) (Myszka, 1999). Therefore, we could rule out that the quenching of the Az fluorescence is due to a dynamic collision. Instead, this fluorescence titration experiment could be indicative of a static quenching, confirming a specific interaction between CytC551 and Az with the involvement of the Az Trp residue. Indeed, the best predicted docking model indicated that the Az hydrophobic patch, which encompasses its Trp48 is in close proximity to the hydrophobic patch of CytC551, as shown in Figure 1(a) (Bizzarri *et al.*, 2007). Moreover, no shift of the maximum emission wavelength (at 308 nm) has been observed.

Copyright © 2014 John Wiley & Sons, Ltd.

Because of the high sensitivity of Trp residues emission to local environment (Lakowicz, 2006), the lack of the Az Trp48 emission shift could either indicate that the Trp48 environment has not been affected by an eventual Az conformational change, or the absence of any conformational change in the complex formation, in agreement with SPR results. Indeed, we recall that the two-state binding model assuming a conformational change of the complex after the interaction does not fit the SPR results.

Fit of the data with Eq. 7 allowed us to estimate a $K_D = 1/K_{SV}$ of $(4.2 \pm 0.2)\cdot 10^{-5}$ M. Such a value falls in between the two values determined by SPR, $K_{D1} = (8.5 \pm 0.7) \cdot 10^{-4}$ M and $K_{D2} = (3.5 \pm 0.3) \cdot 10^{-6}$ M, in the framework of the heterogeneous model. Although such value is again indicative of the formation of a transient complex, the difference could be due to the different conditions of the two experimental setup. Whereas in SPR measurements, the ligand molecules are immobilized on the substrate and the analyte is in solution, in fluorescence experiment, both partners are free in solution, and this could lead to a somewhat different binding response between the two partners. In addition, fluorescence quenching method is able to monitor only the change in the microenvironment of Trp residues. This means that the method does not consider binding sites not involving Trps. Conversely, SPR monitors refractive index change upon binding interaction, and when proteins interact, the signal is generated independently from the binding site localization. It is thus possible that the K_D found in the fluorescence quenching experiment is the weighted average of complexes having different affinity (perhaps encounter and stable final complex) and that the binding sites of these complexes does not always involve Az Trp residue in the interaction. The fact that the kinetic results depend, at least in part, on the experimental technique used, should be taken into account when kinetic data from molecules in solution are extrapolated to immobilized biomolecules, as those reacting in biosensors.

CONCLUSIONS

The study of the interaction between the ET proteins Az and CytC551 by SPR and fluorescence quenching has allowed us to show the formation of a specific complex between the two biomolecules. An analysis of the SPR data in terms of the heterogeneous ligand model indicates that the binding process takes place through two independent reactions likely involving two sites of the Az molecules immobilized on the chip. This result could be traced back to the formation of an encounter complex between partners, which then evolves toward the final, more stable arrangement. However, we cannot rule out that the existence of two binding interactions is the consequence of some heterogeneity in the binding properties of Az randomly immobilized on the chip. The values of the estimated dissociation constants are consistent with the formation of a transient complex in agreement with the ET capability between Az and CytC551. On the other hand, emission fluorescence of the single Az Trp residue upon the addition of CytC551 at increasing concentrations shows the formation of a complex with the involvement of a single binding site close to the Az Trp residue close to the HP of the protein. No shift of Trp 48 emission has been observed after CytC551 binding, this suggesting that there is not a significant conformational change of Az in the complex formation. These results confirm the prediction of previous computational docking and molecular dynamic simulation studies. The K_D value, as determined by fluorescence, reflects a high turnover of the complex again consistent with the transient character of the Az–CytC551 interaction. The fact that the K_D estimated by fluorescence is between the two values determined by SPR could be attributed to the different experimental conditions used in the two cases: in SPR experiment, one of the two partners, Az, is bound to a substrate, whereas in fluorescence, both partners are free in solution. In addition, whereas SPR monitors all the interactions independently from the binding site localization, in fluorescence spectroscopy, only complexes whose formation affect the Trp environment are considered. Such an aspect deserves some interest in the perspective to use these proteins as integrated in bionano devices. In summary, the characterization of the kinetic properties of the Az–CytC551 complex, obtained by SPR and fluorescence, integrates the picture emerging from previous single molecule studies by atomic force spectroscopy (Bonanni *et al*., 2005; Bonanni *et al*., 2006), by providing a more insightful view of the Az–CytC551 interaction. In particular, the kinetics of this complex seems to be consistent with the ET process occurring between Az and CytC551, and this may deserve some interest for possible application in molecular biosensors.

Acknowledgements

This work has been partly supported by a AIRC (Associazione Italiana per la Ricerca sul Cancro) Grant IG 10412 and by a PRIN-MIUR 2009 project (no. 2009WPZM4S).

REFERENCES

Adams DM, Brus L, Chidsey CED, Creager S, Creutz C, Kagan CR, Kamat PV, Lieberman XM, Lindsay S, Marcus RA, Metzger RM, Michel-Beyerle ME, Miller JR, Newton MD, Rolison DR, Sankey O, Schanze KS, Yardley J, Zhu X. 2003. Charge transfer on the nanoscale: current status. *J. Phys. Chem. B* **107**: 6668–6697.

Andolfi L, Cannistraro S. 2005. Conductive atomic force microscopy study of plastocyanin adsorbed on gold electrode. *Surf. Science* **598**: 68–77.

Arcangeli C, Bizzarri AR, Cannistraro S. 1999. Long term molecular dynamics simulations of Azurin: structure, dynamics and functionality. *Biophys. Chem.* **78**: 247–257.

Bizzarri AR, Brunori E, Bonanni B, Cannistraro S. 2007. Docking and molecular dynamics simulation of the azurin-cytochrome c551 electron transfer complex. *J. Mol. Recogn.* **20**: 122–131.

Bizzarri AR. 2011. Steered Molecular dynamics simulations of the electron transfer complex between azurin and cytochrome c551. *J. Phys. Chem. B* **115**: 1211–1219.

Bizzarri AR, Brida D, Santini S, Cerullo G, Cannistraro S. 2012. Ultrafast pump-probe study of the excited-state charge-transfer dynamics in blue copper rusticyanin. *J. Phys. Chem. B* **116**: 4192–4198.

Björquist P, Boström S. 1997. Determination of the kinetic constants of tissue factor/factor VII/factor VIIA and antithrombin/heparin using surface plasmon resonance. *Thromb. Res.* **85**: 225–236.

Bonanni B, Kamruzzahan ASM, Bizzarri AR, Rankl C, Gruber HJ, Hinterdorfer P, Cannistraro S. 2005. Single molecule recognition between cytochrome C 551 and gold-immobilized azurin by force spectroscopy. *Biophys. J.* **89**: 2783–2791.

Bonanni B, Bizzarri AR, Cannistraro S. 2006. Optimized Biorecognition of cytochrome c 551 and azurin immobilized on thiol-terminated monolayers assembled on Au(111) substrates. *J. Phys. Chem. B* **110**: 14574–14580.

Bønding SH, Henty K, Dingley AJ, Brittain T. 2008. The binding of cytochrome c to neuroglobin: a docking and surface plasmon resonance study. *Int. J. Biol. Macromol.* **43**: 295–299.

Borgia A, Gianni S, Brunori M, Travaglini-Allocatelli C. 2008. Fast folding kinetics and stabilization of apo-cytochrome c. *FEBS Lett.* **582**: 1003–1007.

Catimel B, Nerrie M, Lee FT, Scott AM, Ritter G, Welt S, Old LJ, Burgess AW, Nice EC. 1997. Kinetic analysis of the interaction between the

 Copyright © 2014 John Wiley & Sons, Ltd.

monoclonal antibody A33 and its colonic epithelial antigen by the use of an optical biosensor. A comparison of immobilization strategies. *J. Chromatogr. A* **776**: 15–30.
Ceruso MA, Grottesi A, Di Nola A. 2003. Dynamic effects of mutations within two loops of cytochrome c(551) from Pseudomonas aeruginosa. *Proteins* **50**: 222–229.
Cimei T, Bizzarri AR, Cannistraro S, Cerullo G, De Silvestri S. 2002. Vibrational coherence in azurin with impulsive excitation of the LMCT absorption band. *Chem. Phys. Lett.* **362**: 497–503.
Cooper MA. 2003. Label-free screening of bio-molecular interactions. *Anal. Bioanal. Chem.* **377**: 834–842.
Crowley PB, Ubbink M. 2003. Close encounters of the transient kind: protein interactions in the photosynthetic redox chain investigated by NMR spectroscopy. *Acc. Chem. Res.* **36**: 723–730.
Cutruzzolà F, Arese M, Ranghino G, Van Pouderoyen G, Canters G, Brunori M. 2002. Pseudomonas aeruginosa cytochrome C-551: probing the role of the hydrophobic patch in electron transfer. *J. Inorg. Biochem.* **88**: 353–361.
De Crescenzo G, Grothe S, Lortie R, Debanne MT, O'Connor-McCourt M. 2000. Real-time kinetic studies on the interaction of transforming growth factor alpha with the epidermal growth factor receptor extracellular domain reveal a conformational change model. *Biochemical* **39**: 9466–9476.
Delfino I, Cannistraro S. 2009. Optical investigation of the electron transfer protein azurin-gold nanoparticle system. *Biophys. Chem.* **139**: 1–7.
Gorton L, Lindgren A, Larsson T, Munteanu FD, Ruzgas T, Gazaryan I. 1999. Direct electron transfer between heme-containing enzymes and electrodes as basis for third generation biosensors. *Anal. Chim. Acta* **400**: 91–108.
Goto M, Yamada T, Kimbara K, Horner J, Newcomb M, Das Gupta TK, Chakrabarty AM. 2003. Induction of apoptosis in macrophages by Pseudomonas aeruginosa azurin: tumour-suppressor protein p53 and reactive oxygen species, but not redox activity, as critical elements in cytotoxicity. *Mol. Microbiol.* **47**: 549–559.
Gray HB, Winkler JR. 1996. Electron transfer in proteins. *Ann. Rev. Biochem.* **65**: 537–561.
Guo S, Dong S. 2009. Biomolecule-nanoparticle hybrids for electrochemical biosensors. *Trends Anal. Chem.* **28**: 96–109.
Hasegawa J, Shimahara H, Mizutani M, Uchiyama S, Arai H, Ishii M, Kobayashi Y, Ferguson SJ, Sambongi Y, Igarashi Y. 1999. Stabilization of Pseudomonas aeruginosa cytochromec 551 by systematic amino acid substitutions based on the structure of thermophilic hydrogenobacter thermophilus cytochrome c 552. *J. Biol. Chem.* **274**: 37533–37537.
Hiraoka Y, Yamada T, Goto M, Das Gupta TK, Chakrabarty AM. 2004. Modulation of mammalian cell growth and death by prokaryotic and eukaryotic cytochrome c. *Proc. Natl. Acad. Sci. U. S. A.*. **101**: 6427–6432.
Homola J, Yee SS, Gauglitz G. 1999. Surface plasmons resonance sensors: review. *Sens. Actuators B* **54**: 3–15.
Jain KK. 2005. Nanotechnology in clinical laboratory diagnostics. *Clin. Chim. Acta* **358**: 37–54.
Janin J. 2000. Kinetics and thermodynamics of protein-protein interactions. In Protein–Protein Recognition. Oxford University Press: New York.
Karlsson R. 1994. Real-time competitive kinetic analysis of interactions between low-molecular-weight ligands in solution and surface-immobilized receptors. *Anal. Biochem.* **221**: 142–151.
Karlsson R, Katsamba PS, Nordin H, Pol E, Myszka DG. 2006. Analyzing a kinetic titration series using affinity biosensors. *Anal. Biochem.* **349**: 136–147.
Lakowicz JR. 1999. Principles of Fluorescence Spectroscopy, 2nd edn. Plenum Press: New York.
Lakowicz JR. 2006. Principles of Fluorescence Spectroscopy, 3rd edn. Springer: New York.
Liu B, Chen Y, St. Clair DK. 2008. ROS and p53: versatile partnership. *Free Radical Bio. Med.* **44**: 1529−1535.
Marcus RA, Sutin N. 1985. Electron transfer in chemistry and biology. *Biochim. Biophys. Acta* **811**: 265–322.
Marvin JS, Hellinga HW. 2001. Conversion of a maltose receptor into a zinc biosensor by computational design . *Proc. Natl. Acad. Sci. U. S. A.* **98**: 4955–4960.
Matsuura Y, Takano T, Dickerson RE. 1982. Structure of cytochrome c551 from Pseudomonas aeruginosa refined at 1.6. A resolution and comparison of the two redox forms. *J. Mol. Biol.* **156**: 389–409.
Morton TA, Myszka DG, Chaiken IM. 1995. Interpreting complex binding kinetics from optical biosensors: a comparison of analysis by linearization, the integrated rate equation, and numerical integration. *Anal. Biochem.* **227**: 176–185.
Myszka DG. 1999. Improving biosensor analysis. *J. Mol. Recognit.* **12**: 279–284.
Nar H, Messerschmidt A, Huber R, Van de Kamp M, Canters GW. 1991. Crystal structure analysis of oxidized Pseudomonas aeruginosa azurin at pH 5.5 and pH 9.0. A pH-induced conformational transition involves a peptide bond flip. *J. Mol. Biol.* **221**: 765–772.
Nooren IM, Thornton JM. 2003. Structural characterisation and functional significance of transient protein–protein interactions. *J. Mol. Biol.* **325**: 991–1018.
O'Shannessy DJ, Brigham-Burke M, Soneson KK, Hensley P, Brooks I. 1993. Determination of rate and equilibrium binding constants for macromolecular interactions using surface plasmon resonance: use of nonlinear least squares analysis methods. *Anal. Biochem.* **212**: 457–468.
O'Shannessy DJ, Winzor DJ. 1996. Interpretation of deviations from pseudo-first-order kinetic behavior in the characterization of ligand binding by biosensor technology. *Anal. Biochem.* **236**: 275–283.
Prabhulkar S, Tian H, Wang X, Zhu JJ, Li CZ. 2012. Engineered proteins: redox properties and their applications. *Antioxid. Redox Signal.* **17**: 1796–1822.
Schasfoort RBM, Tudos AJ. 2008. Handbook of Surface Plasmon Resonance. Royal Society of Chemistry: London.
Silvestrini MC, Tordi MG, Colosimo A, Antonini E, Brunori M. 1982. The kinetics of electron transfer between Pseudomo-nas aeruginosa cytochrome c-551 and its oxidase. *Biochem. J.* **203**: 445–451.
Solomon EI, Baldwin MJ, Lowery MD. 1992. Electronic structure of active sites in copper proteins: contributions to reactivity. *Chem. Rev.* **92**: 521–542.
Sykes AG. 1991. Active-site properties of the blue copper proteins. *Adv. Inorg. Chem.* **36**: 377–408.
Taranta M, Bizzarri AR, Cannistraro S. 2008. Probing the interaction between p53 and the bacterial protein azurin by single molecule force spectroscopy. *J. Mol. Recognit.* **21**: 63−70.
Turoverov KK, Kuznetsova IM, Zaitsev VN. 1985. The environment of the tryptophan residue in Pseudomonas aeruginosa azurin and its fluorescence properties. *Biophys. Chem.* **23**: 79–89.
Ubbink M. 2009. The courtship of proteins: understanding the encounter complex. *FEBS Lett.* **583**: 1060–1066.
Webb MA, Loppnow GRA. 1999. Structural basis for long-range coupling in azurins from resonance Raman spectroscopy. *J. Phys. Chem. A* **103**: 6283–6287.
Willner I, Willner B. 2001. Biomaterials integrated with electronic elements: en route to bioelectronics. *Trends Biotechnol.* **19**: 222–230.
Wilson MT, Greenwood C, Brunori M, Antonini E. 1975. Electron transfer between azurin and cytochrome c-551. *Biochem. J.* **145**: 449–457.
Yamada T, Goto M, Punj V, Zaborina O, Chen ML, Kimbara K, Majumdar D, Cunningham E, Das Gupta TK, Chakrabarty AM. 2002. Bacterial redox protein azurin, tumor suppressor protein p53, and regression of cancer. *Proc. Natl. Acad. Sci. U.S.A.* **99**: 14098–14103.
Zannoni D. 1989. The respiratory chains of pathogenic pseudomonas. *Biochim. Biophys. Acta* **975**: 299–316.

Copyright © 2014 John Wiley & Sons, Ltd.